Title: Quantitative Optical Coherence Tomography Angiography of Radial Peripapillary Capillaries in Glaucoma, Glaucoma Suspect and Normal Eyes

Short title: OCT Angiography of Peripapillary Capillaries in Glaucoma

Authors: Zaid Mammo[1]
Morgan Heisler[2]
Chandrakumar Balaratnasingam[1,3,4,5]
Sieun Lee[2]
Dao-Yi Yu[5]
Paul Mackenzie[1,2]
Steven Schendel[1]
Andrew Merkur[1]
Andrew Kirker[1]
David Albiani[1]
Eduardo Navajas[1]
Mirza Faisal Beg[2]
William Morgan[5]
Marinko V. Sarunic[2]

1: Department of Ophthalmology and Visual Sciences, University of British Columbia, 2550 Willow Street, Vancouver, V5Z 3N9, British Columbia, Canada
2: School of Engineering Science, Simon Fraser University, 8888 University Drive, Burnaby, V5A 1S6, British Columbia, Canada
3: Vitreous Retina Macula Consultants of New York, 460 Park Avenue, 5th Floor, New York 10022, New York, United States
4: Luesther T. Mertz Retinal Research Center, Eye, Ear and Throat Hospital, 210 East 64th Street, New York, 10065, New York, United States
5: Department of Physiology and Pharmacology, Centre for Ophthalmology and Visual Science, Lions Eye Institute, The University of Western Australia, 2 Verdun Street, Nedlands, 6009, Western Australia, Australia

Corresponding Author:
Marinko V. Sarunic, PhD
School of Engineering Science,
Simon Fraser University,
8888 University Drive,
Burnaby, V5A 1S6,
British Columbia
Tel: (778) 782-7654
Fax: (778) 782-4951
Email: msarunic@sfu.ca

Introduction

Glaucoma is a leading cause of irreversible blindness worldwide[1] and the second most common cause of blindness in the developed world.[2] The pathophysiology of glaucoma is complex and characterized by the time-dependent loss of retinal ganglion cells (RGCs) and their accompanying axons.[3] Indices that are currently used to quantify and evaluate progression of glaucomatous optic neuropathy include visual field testing, nerve fibre layer (NFL), optic nerve head[4], ganglion cell layer with inner plexiform layer (GCIPL) and ganglion cell complex parameters analysis.[5] The nutritional demands of RGC axons are likely to be partially satisfied by radial peripapillary capillaries (RPCs)[6-9] and structural changes to RPCs have been implicated in the pathogenesis of Bjerrum scotoma[10] and glaucoma.[11] The RPCs represent a unique capillary plexus within the inner aspect of the NFL.[12] They are largely restricted to the posterior pole of the human retina along specific retinal eccentricities surrounding the optic nerve. Morphologically, this capillary network display minimal inter-capillary anastomosis and show a linear course in keeping with the NFL distribution. The anatomical distribution and unique morphological characteristics help to distinguish the RPCs from other capillary plexuses within the retinal microcirculation.[13] Despite the evidence that RPCs are critically related to RGC function[7,12,13], the morphological characteristics of RPCs are not routinely used in clinical practice to evaluate glaucomatous progression. This may be because RPCs are not reliably visualized with fluorescein angiography (FA)[14] which is the mainstay imaging modality for clinically evaluating the retinal circulation.

Optical coherence tomography angiography (OCT-A) is a relatively new, non-invasive imaging technique that utilizes flow-based information to visualize the retinal and optic disc circulation.[15] Our previous studies evaluated the morphological characteristics of the foveal[16], perifoveal[17] and peripapillary capillary[9] networks using speckle variance (sv) OCT-A[18] and showed that the topological and quantitative characteristics of these networks, as seen on OCT-A, are comparable to histologic representation. This report utilizes OCT-A to quantitatively evaluate RPCs in glaucoma, glaucoma suspects and normal eyes. Correlations between RPC density, NFL thickness and visual field index (VFI) provided in this study suggest that the quantitative characteristics of RPCs may be a useful metric for evaluating RGC axonal loss in glaucoma.

Methods

The research work was conducted as a cross-sectional study. All subject recruitment and imaging took place at the Eye Care Centre at Vancouver General Hospital. The study protocol including subject recruitment and imaging was approved prospectively by the Research Ethics Boards at the University of British Columbia and Vancouver General Hospital. The study was performed in accordance and adhered with the tenets of the Declaration of Helsinki. Written informed consent was obtained from all subjects.

Inclusion Criteria and Subject Recruitment

A total of 32 eyes from 17 subjects were imaged with OCT-A. This included 10 eyes from 5 subjects in Group A, 6 eyes from 3 subjects in Group B and 16 eyes from 9 subjects in Group C. Group A consisted of subjects with unilateral glaucomatous optic neuropathy and a normal fellow eye. Eyes with glaucomatous optic neuropathy met all

of the following criteria: 1) Evidence of optic disc neural rim loss on clinical examination; 2) Evidence of peripapillary NFL loss on spectral-domain optical coherence tomography (SD-OCT). 3) Glaucomatous pattern of visual field defect on automated Humphrey Visual Field (HVF) Testing (30-2) with an abnormal pattern standard deviation ($P<0.05$). 4) Stable SD-OCT, HVF and optic disc clinical examination for 6 or more months.

Group B consisted of glaucoma suspects. Eyes in this group met the following criteria: 1) No evidence of progressive optic disc neural rim loss on clinical examination; 2) Evidence of non-progressive NFL thinning in at least one region on SD-OCT for at least 12 months; 3) Normal baseline 30-2 HVF test with normal Visual Field Index (VFI) and pattern standard values; and 4) No clinical history of: i) Unexplained optic disc hemorrhage, ii) Family history of glaucoma, iii) Intraocular pressure measurement above 21mmHg, iv) Central corneal thickness below 500 µm, or v) History of non-glaucomatous optic neuropathy or retinal pathology.

Group C was the normal control group with no evidence of retinal or optic nerve pathology. Quantitative and morphological RPC analysis of imaging from this group has been previously published.[9]

Visual Fields, Disc Photographs, Peripapillary Optical Coherence Tomography

Visual fields were acquired using the Humphrey Field Analyzer II (Carl Zeiss Meditec, Dublin, CA). The settings were set for 30-2 threshold test, standard SITA protocol. Refractive error was corrected during testing. The maximum false positive or false negative value was set at 10%, and a maximum of three instances of fixation loss was chosen. Stereoscopic photos around the optic discs were obtained for each participant using a fundus camera (TRC-50DX; Topcon, Japan) with 5.0-megapixel resolution. Peripapillary assessment of the NFL was done using the standard peripapillary protocol using SD-OCT (Spectralis, Heidelberg Engineering, Germany). All ancillary testing were acquired within six months of speckle variance OCT-A imaging.

Optical Coherence Tomography Angiography Instrumentation

Speckle variance OCT-A images and simultaneous, co-registered regular structural OCT images were acquired from a GPU-accelerated OCT clinical prototype. The details of the acquisition system have previously been published.[18] The OCT system uses a 1060nm swept source (Axsun Inc.) with 100 kHz A-scan rate and a full-width half-maximum bandwidth of 61.5nm which corresponds to a coherence length of ~6µm in tissue. For the speckle variance calculation, three repeat acquisitions were obtained at each B-scan location. The scan area was sampled in a 300x300(x3) grid with a ~2x2mm field of view in 3.15 seconds. Scan dimensions were calibrated based on the eye length of each participant, measured using the IOL Master 500 (Carl Zeiss Meditec Inc., Dublin, California, USA). Processing of the OCT intensity image data and *en face* visualization of the retinal microvasculature was performed in real time using our open source code for alignment and quality control purposes.[19,20]

Processing of OCT-A Images

Post-processing of the raw intensity data was performed to segment the retinal layers and extract optimal quality images of the retinal microvasculature. Coarse axial motion artifact was corrected using cross-correlation between adjacent frames. Sub-pixel registration was performed on each set of corresponding B-scans before creating the speckle variance B-mode scan. Before layer segmentation, three-dimensional bounded variance smoothing was applied to the motion corrected intensity images in order to reduce the effect of speckle while preserving and enhancing edges. The inner limiting membrane, posterior boundary of the NFL, inner nuclear layer and outer nuclear layer were segmented automatically in 3D using a graph-cut algorithm.[21] The automated segmentation was examined and corrected by a trained grader using Amira (version 5.1; Visage Imaging, San Diego, CA, USA). The OCT-A image within each layer was summed in the axial direction to produce a projected *en face* image. *En face* images were notch filtered and contrast-adjusted using adaptive histogram equalization. In an effort to eliminate the bias of large blood vessels from the NFL thickness measurement, the images were cropped to an area of ~1x1mm to remove the majority of the large blood vessels present. Furthermore, prior to performing capillary density comparisons between glaucoma, glaucoma suspect and normal control subjects the images were again cropped to an area of 636.5x636.5μm.

Image Acquisition and Quantification

The 8 peripapillary regions imaged with speckle variance OCT-A are illustrated in Figure 1. In Group A, the peripapillary region that was associated with the site of focal optic disc rim defect and corresponding HVF loss and NFL thinning was imaged first. A matched region in the normal fellow eye was then imaged. In Group B, the peripapillary region that was associated with the site of lowest NFL thickness, as determined using SD-OCT, was imaged with OCT-A. Region selection for OCT-A imaging in Group A and B subjects was agreed upon collectively by ZM, MH, SL and CB. In group C, all 8 peripapillary regions were imaged with speckle variance OCT-A as has been previously reported.[9]

Our previously published manual tracing technique was used to quantify RPC density as shown in Figure 2.[16] Manual tracing was performed using the GNU Image Manipulation Program Version 2.8.14. All manual tracings were performed by ZM in a non-blinded fashion. Care was taken to trace RPCs, and all large vessels originating from the disc were segmented separately and excluded. Capillary density was measured in the segmented image using MATLAB. The proportion of the image occupied by retinal vessels was expressed as a percentage, and the unit of measurement was calculated as the percentage retinal area occupied by capillary plexus. As speckle variance images are derived from the structural intensity scans, quantitative structural information such as the NFL thickness can be extracted from the exact same location as capillary density. The NFL thickness was measured and averaged across the cropped volumetric ~1x1mm scan of the region of interest. Where reported, the density of the RPCs was calculated as the fraction of pixels identified as belonging to a vessel versus the total number of pixels in an image. To determine the reproducibility of these measurements, three images from Group A, B and C were

manually traced and quantified on two separate occasions in a blinded fashion, each at least 3 months apart, by the same rater, ZM. To facilitate the qualitative comparisons of the deep capillary plexus, careful manual segmentation of the retinal layers was performed to minimize projection artifacts. In addition, manually scrolling through the entire OCT volume helped to identify and exclude any residual projection artifacts from the overlying large superficial vessels in the qualitative comparison. The unique morphological appearance of multiple closed loops in a laminar configuration was used as the guiding principle for identification and assessment of the deep capillary plexus.[6]

Statistical Analysis

Inter-group mean comparisons were done using one-way ANOVA. Prior to group comparisons, the assumption of homogeneity of variances was tested using Levene's Test. A linear mixed regression model incorporating the random effects on the scale of the linear predictor was used with capillary density as the response variable. The covariate tested wasNFL thickness . The random effects were 'eye' (right or left) to account for measurement from both eyes of the same individual, nested within 'subject' to account for some multiple measurements from the same eye. The Q-Q normal plot showed normal distribution of the data across the mean. Statistical analysis was performed using R [R Core Team (2013). R: A language and environment for statistical computing. R Foundation for statistical computing, Vienna, Austria. URL http://www.R-project.org/.]. Statistical significance was set as $P<0.05$.

Results

The average age of subjects (range and median) of Groups A, B and C were 58.00±18.60 (26-72: 66) years, 44.67±23.50 years (21-68: 45) and 41.13±13.51 years (27-60: 36), respectively (P=0.25). The male: female ratio of subjects in Group A, B and C were 3:2, 3:0 and 4:3, respectively. The average intraocular pressure of subjects (range and median) of the glaucoma eyes and fellow eyes in Group A and Group B were 11.46 ± 4.21 mmHg (5-15: 12), 13.74 ± 3.21 mmHg (10-17: 14) and 16.17 ± 2.04 mmHg (14-19: 16), respectively.

Morphology of RPCs and the Deeper Retinal Networks

In the normal control group, the RPCs followed a very similar trajectory to the RGC axons in the NFL and demonstrated a linear course with minimal anastomoses. Decreased density of RPCs was observed within regions of optic disc neural rim loss in glaucomatous eyes. In glaucomatous eyes, RPCs maintained a linear trajectory, however a patchy or diffuse loss of RPCs was observed within regions of NFL thinning. The density and morphologic characteristics of deeper capillary networks, beyond the outer margins of the NFL, at sites of RPC loss appeared normal in glaucomatous eyes (Figure 3).

Inter-Group Comparisons of RPC Density and NFL Thickness

The mean density of RPCs at sites of NFL thinning and disc rim change in glaucomatous eyes was 0.09 ± 0.05 of total tissue area. The density of RPCs in the matched region of fellow eyes in these patients was significantly greater [0.30 ± 0.06 of total tissue area; (P < 0.001)]. The mean density of RPCs for the glaucoma suspect eyes in Group B and normal control eyes in Group C were 0.28±0.01 and 0.33±0.04 of total tissue area, respectively. The density of RPCs in glaucomatous eyes was significantly lower than glaucoma suspect and normal control eyes (both P < 0.001). No other statistically significant inter-group differences in RPC density were identified. There was no significant difference (P=0.81) between capillary density of the randomly selected nine images (3 from each group) that underwent repeat tracing at different time points.

The average (range and median) NFL thickness at sites of NFL thinning and disc rim change in glaucomatous eyes was 42.84±15.93 µm (30-60.30: 33). The NFL thickness at matched sites in the fellow eye of these patients was 74.68±16.80 µm (55.10-97.80: 72.10). The average NFL thickness for eyes in Group B and Group C were 63.50±31.32 µm (50.10-133.60: 72.80) and 102.70±35.56 µm (52.92-153.25: 99.24), respectively. The NFL thickness values were significantly lower in glaucomatous eyes in Group A when compared to the normal control eyes in Group C (P=0.005). No other statistically significant differences in mean NFL thickness values were found on inter-group comparisons.

Correlations between RPC density, NFL thickness and VFI

A plot of RPC density and NFL thickness using pooled data from all groups is presented in Figure 4. A univariate model, accounting for multiple measures from each subject demonstrated a significant correlation between RPC density and NFL thickness (P<0.0001 and Slope=0.0010).

The average VFI (range and median) of the glaucomatous eyes in group A, fellow eyes in group A and glaucoma suspect eyes in group B were 69.80 ± 13.33% (56-90: 67), 98.8 ± 2.2% (95-100: 100) and 99.2 ± 1.2% (97-100: 100), respectively. A plot of RPC density and VFI values is provided in Figure 5. Only subjects in Groups A and B were used for this analysis. A significant correlation was found between RPC density and VFI value (P=0.001 and Slope=0.006).

Discussion

The quantitative characteristics of RPCs in glaucoma, glaucoma suspect and normal control eyes were evaluated in this study using speckle variance OCT-A. The major findings are as follows: 1) Glaucomatous optic neuropathy is characterized by selective loss of radial peripapillary capillaries at sites of RGC axonal loss, NFL thinning, and disc rim changes; (2) RPC density is strongly correlated to NFL thickness; and 3) RPC density is strongly correlated to VFI values.

Radial peripapillary capillaries comprise a unique vascular plexus that is predominantly found in the posterior pole of primates with a typical macula.[7] As the metabolic demands of RGC axons are likely to be partially met by the RPCs[6-9], they are vulnerable to vasogenic insults. Structural changes to the RPC network has been implicated in the

pathogenesis of age-related RGC axonal loss, cotton wool spots[22] and Bjerrum scotomas.[10] There is also evidence to demonstrate an association between RPC loss and NFL changes in chronic glaucoma.[11] Although clinical imaging of RPCs may be a potentially useful way for evaluating and monitoring RGC axonal disease, it is not routinely used in clinical practice due to the difficulties associated with visualizing this circulation using FA.[14] Our previous study showed that quantitative analysis of retinal capillary detail could only be performed in 30% of FA images acquired from normal subjects with clear ocular media. The major limiting factor that precludes clear visualization of retinal capillaries on FA is fluorescence from the choroidal circulation.[23] Our recent studies have quantified the morphological characteristics of retinal capillary networks as seen OCT-A and have shown that it is comparable to histological representation[9,16,17] thus suggesting that OCT-A techniques may be useful for evaluating the structural characteristics of retinal capillary networks.

Optical coherence tomography angiography overcomes some of the limitations of FA as it is a label-free technique that permits non-invasive, depth-resolved evaluation of retinal capillary networks.[15] The advantages of OCT-A techniques have recently been used to improve our understanding of the pathogenic relationships between the optic disc circulation and the process of glaucomatous axonal loss. The recent OCT-A studies investigating the optic disc and peripapillary perfusion employed Split Spectrum Amplitude Decorrelation Algorithm (SSADA)[24] for extracting angiography information from OCT data. Our group has been using speckle variance OCT-A[25], a sister technology to SSADA. In short, the speckle variance method utilizes the variance of the amplitude fluctuations between B-scans to visualize flow-based information. On the other hand, the SSADA technique is based on splitting interference spectrum into narrower bands from which the decorrelation is then calculated and averaged. An overview of the different OCT-A technologies could be found in some of the recently published reviews in the field.[26] Jia et al utilized SSADA OCT-Angiography to compare the optic nerve head perfusion in normal and glaucoma subjects.[27] The authors calculated an ‘optic disc perfusion index’ which was found to be correlated with the visual field pattern standard deviation values. By performing an 8x8mm scan centred around the optic disc, Liu et al were able to estimate the combined optic nerve head and the peripapillary area perfusion through calculating an ‘optic disc perfusion peripapillary index’. The authors demonstrated reduced peripapillary flow and capillary density in glaucomatous eyes compared to normal eyes. Their analysis comprised the entire peripapillary circulation, including superficial and deeper capillaries as well as the large-calibre vessels ranging from the ILM to the RPE.[28] Another study, similar in its design and findings to that of Liu et al, was recently published by Wang et al.[29] In contrast to those studies, our quantitative analysis was based on the careful segmentation and manual tracing of the RPC network only, deeper capillaries were only compared qualitatively. In addition, we employed manual tracing techniques to calculate the RPC network density and showed that glaucoma is characterized by a significant and preferential reduction in RPC density. As shown in Figure 3, focal and diffuse patterns of RPC loss were identified in the NFL in glaucomatous eyes while the deeper capillary networks appeared structurally normal.

Univariate analysis with linear mixed modelling showed that RPC density was strongly correlated with NFL thickness and also VFI. With respect to NFL thickness, our findings support the conclusion previously reached by Jia et al. who demonstrated a significant correlation between peripapillary perfusion index values and NFL thickness in subjects with glaucoma.[30] Regarding VFI values, our results are consistent with the findings of recent studies that have shown a correlation between optic disc blood flow index values and the degree of visual field loss in glaucoma subjects.[30-32] Collectively, the results of our study suggest that measures of RPC density may be useful, in conjunction with NFL thickness and VFI, for quantifying the degree of RGC axonal loss in glaucoma. Quantifying RPC density may be a particularly useful technique for assessing patients with anomalous optic discs where it may be difficult to reliably distinguish between intraocular pressure-induced neural rim changes and congenital variation.[33,34] Evaluation of the myopic optic disc can pose a clinical challenge in certain contexts and quantification of RPC density may be particularly useful for aiding the determination of glaucomatous changes in tilted discs, microdiscs and macrodiscs.

This exploratory study demonstrates important correlations between RPC density, NFL thickness and VFI. A limitation of this study includes the restricted sample size however this limitation was accounted for in the statistical analysis that was used to compare differences between groups. The small sample size prevented our ability to test for the effect of possible covariates in our univariate analysis. The small sample size could explain the lack of a statistically significant difference between the mean ages of the groups. Manual tracing techniques were used to calculate RPC density and we acknowledge that in order for this technique to have broad clinical utility an automated method for determining RPC density will be required. Skeletonization algorithms and binary image analysis techniques may potentially overcome this limitation. All manual tracings were performed by ZM in a non-blinded fashion. To minimize grader bias, all tracings were collectively reviewed and approved by ZM, MH and CB prior to analysis. As outlined in the methods section, a number of manual steps were taken to minimize the potential deleterious effects of projection artifacts from overlying vessels on our qualitative comparison of the deep capillary networks between the study groups. This topic is receiving increased attention in the OCTA literature, and automated methods for removing projection artifacts are still in the development phase.[35] Finally, we emphasize that only a single time point was evaluated in this study and therefore the results of this work cannot be used to determine cause-effect relationships in glaucoma. Longitudinal evaluation of patients and temporal correlation of NFL, VFI and RPC changes will help clarify relationships between vascular changes and RGC axonal loss in glaucomatous optic neuropathy.

Acknowledgements/Disclosure:

A. Funding was received from the following sources:

1. Michael Smith Foundation for Health Research, Vancouver, Canada
2. Natural Sciences and Engineering Research Council of Canada, Ottawa, Canada
3. Canadian Institutes of Health Research and National Health, Ottawa, Canada
4. Brain Canada, Montreal, Canada
5. LuEsther T. Mertz Retinal Research Center, Manhattan Eye, Ear and Throat Hospital, New York, NY, USA
6. The Macula Foundation, Inc., New York, NY, USA.
7. National Health and Medical Research Council of Australia, Nedlands, Australia

The funding sources had no role in any aspect of the design or conduct of this research or the decision to publish. This work is original and has not been published elsewhere.

B. Financial disclosures: Marinko Sarunic: Netra Systems Inc. (Consulting). All other authors have no financial disclosures

C. Other Acknowledgements: None

References:

1. Tham YC, Li X, Wong TY, Quigley HA, Aung T, Cheng CY. Global prevalence of glaucoma and projections of glaucoma burden through 2040: A systematic review and meta-analysis. *Ophthalmology*. 2014;121(11):2081-2090.
2. Quigley HA, Broman AT. The number of people with glaucoma worldwide in 2010 and 2020. *Br J Ophthalmol*. 2006;90(3):262-267.
3. Kwon YH, Fingert JH, Kuehn MH, Alward WL. Primary open-angle glaucoma. *N Engl J Med*. 2009;360(11):1113-1124.
4. Chauhan BC, O'Leary N, Almobarak FA, et al. Enhanced detection of open-angle glaucoma with an anatomically accurate optical coherence tomography-derived neuroretinal rim parameter. *Ophthalmology*. 2013;120(3):535-543.
5. Bussel II, Wollstein G, Schuman JS. OCT for glaucoma diagnosis, screening and detection of glaucoma progression. *Br J Ophthalmol*. 2014;98 Suppl 2:ii15-9.
6. Yu PK, Cringle SJ, Yu DY. Correlation between the radial peripapillary capillaries and the retinal nerve fibre layer in the normal human retina. *Exp Eye Res*. 2014;129:83-92.
7. Henkind P. Symposium on glaucoma: Joint meeting with the national society for the prevention of blindness. new observations on the radial peripapillary capillaries. *Invest Ophthalmol*. 1967;6(2):103-108.
8. Scoles D, Gray DC, Hunter JJ, et al. In-vivo imaging of retinal nerve fiber layer vasculature: Imaging histology comparison. *BMC Ophthalmol*. 2009;9:9-2415-9-9.
9. Yu PK, Balaratnasingam C, Xu J, et al. Label-free density measurements of radial peripapillary capillaries in the human retina. *PLoS One*. 2015;10(8):e0135151.
10. Alterman M, Henkind P. Radial peripapillary capillaries of the retina. II. possible role in bjerrum scotoma. *Br J Ophthalmol*. 1968;52(1):26-31.
11. Kornzweig AL, Eliasoph I, Feldstein M. Selective atrophy of the radial peripapillary capillaries in chronic glaucoma. *Arch Ophthalmol*. 1968;80(6):696-702.
12. Yu PK, Cringle SJ, Yu DY. Correlation between the radial peripapillary capillaries and the retinal nerve fibre layer in the normal human retina. *Exp Eye Res*. 2014;129:83-92.
13. Henkind P. Radial peripapillary capillaries of the retina. I. anatomy: Human and comparative. *Br J Ophthalmol*. 1967;51(2):115-123.
14. Spaide RF, Klancnik JM,Jr, Cooney MJ. Retinal vascular layers imaged by fluorescein angiography and optical coherence tomography angiography. *JAMA Ophthalmol*. 2015;133(1):45-50.
15. Zhang A, Zhang Q, Chen CL, Wang RK. Methods and algorithms for optical coherence tomography-based angiography: A review and comparison. *J Biomed Opt*. 2015;20(10):100901.
16. Mammo Z, Balaratnasingam C, Yu P, et al. Quantitative noninvasive angiography of the fovea centralis using speckle variance optical coherence tomography. *Invest Ophthalmol Vis Sci*. 2015;56(9):5074-5086.
17. Chan G, Balaratnasingam C, Xu J, et al. In vivo optical imaging of human retinal capillary networks using speckle variance optical coherence tomography with quantitative clinico-histological correlation. *Microvasc Res*. 2015;100:32-39.
18. Xu J, Han S, Balaratnasingam C, et al. Retinal angiography with real-time speckle variance optical coherence tomography. *Br J Ophthalmol*. 2015;99(10):1315-1319.

19. Jian Y, Wong K, Sarunic MV. Graphics processing unit accelerated optical coherence tomography processing at megahertz axial scan rate and high resolution video rate volumetric rendering. *J Biomed Opt*. 2013;18(2):26002.
20. Xu J, Wong K, Jian Y, Sarunic MV. Real-time acquisition and display of flow contrast using speckle variance optical coherence tomography in a graphics processing unit. *J Biomed Opt*. 2014;19(2):026001.
21. Lee S, Fallah N, Forooghian F, et al. Comparative analysis of repeatability of manual and automated choroidal thickness measurements in nonneovascular age-related macular degeneration. *Invest Ophthalmol Vis Sci*. 2013;54(4):2864-2871.
22. Ashton N. Pathophysiology of retinal cotton-wool spots. *Br Med Bull*. 1970;26(2):143-150.
23. Mendis KR, Balaratnasingam C, Yu P, et al. Correlation of histologic and clinical images to determine the diagnostic value of fluorescein angiography for studying retinal capillary detail. *Invest Ophthalmol Vis Sci*. 2010;51(11):5864-5869.
24. Jia Y, Morrison JC, Tokayer J, et al. Quantitative OCT angiography of optic nerve head blood flow. *Biomed Opt Express*. 2012;3(12):3127-3137.
25. Mariampillai A, Standish BA, Moriyama EH, et al. Speckle variance detection of microvasculature using swept-source optical coherence tomography. *Opt Lett*. 2008;33(13):1530-1532.
26. Zhang A, Zhang Q, Chen CL, Wang RK. Methods and algorithms for optical coherence tomography-based angiography: A review and comparison. *J Biomed Opt*. 2015;20(10):100901.
27. Jia Y, Wei E, Wang X, et al. Optical coherence tomography angiography of optic disc perfusion in glaucoma. *Ophthalmology*. 2014;121(7):1322-1332.
28. Liu L, Jia Y, Takusagawa HL, et al. Optical coherence tomography angiography of the peripapillary retina in glaucoma. *JAMA Ophthalmol*. 2015;133(9):1045-1052.
29. Wang X, Jiang C, Ko T, et al. Correlation between optic disc perfusion and glaucomatous severity in patients with open-angle glaucoma: An optical coherence tomography angiography study. *Graefes Arch Clin Exp Ophthalmol*. 2015;253(9):1557-1564.
30. Jia Y, Wei E, Wang X, et al. Optical coherence tomography angiography of optic disc perfusion in glaucoma. *Ophthalmology*. 2014;121(7):1322-1332.
31. Liu L, Jia Y, Takusagawa HL, et al. Optical coherence tomography angiography of the peripapillary retina in glaucoma. *JAMA Ophthalmol*. 2015;133(9):1045-1052.
32. Wang X, Jiang C, Ko T, et al. Correlation between optic disc perfusion and glaucomatous severity in patients with open-angle glaucoma: An optical coherence tomography angiography study. *Graefes Arch Clin Exp Ophthalmol*. 2015;253(9):1557-1564.
33. Chang RT, Singh K. Myopia and glaucoma: Diagnostic and therapeutic challenges. *Curr Opin Ophthalmol*. 2013;24(2):96-101.
34. Aref AA, Sayyad FE, Mwanza JC, Feuer WJ, Budenz DL. Diagnostic specificities of retinal nerve fiber layer, optic nerve head, and macular ganglion cell-inner plexiform layer measurements in myopic eyes. *J Glaucoma*. 2014;23(8):487-493.
35. Zhang A, Zhang Q, Wang RK. Minimizing projection artifacts for accurate presentation of choroidal neovascularization in OCT micro-angiography. *Biomed Opt Express*. 2015;6(10):4130-4143.

Figure Legends

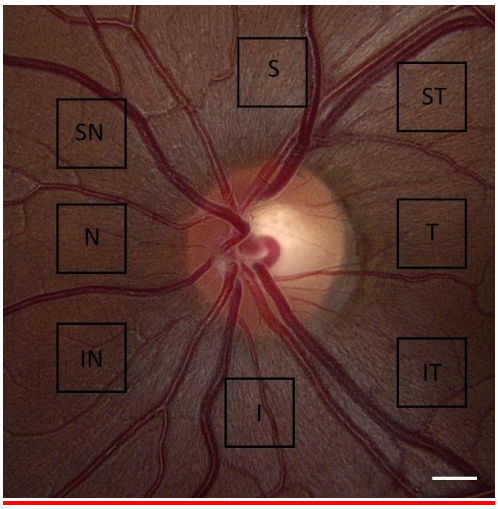

Figure 1 – **Regions of interest**. The 8 peripapillary regions where the density of radial peripapillary capillaries were evaluated using speckle variance OCT-A are illustrated. S=Superior, ST=Superotemporal, T=Temporal, IT=Inferotemporal, I=Inferior, IN=Inferonasal, N=Nasal, SN=Superonasal. Scale bar = 500 µm.

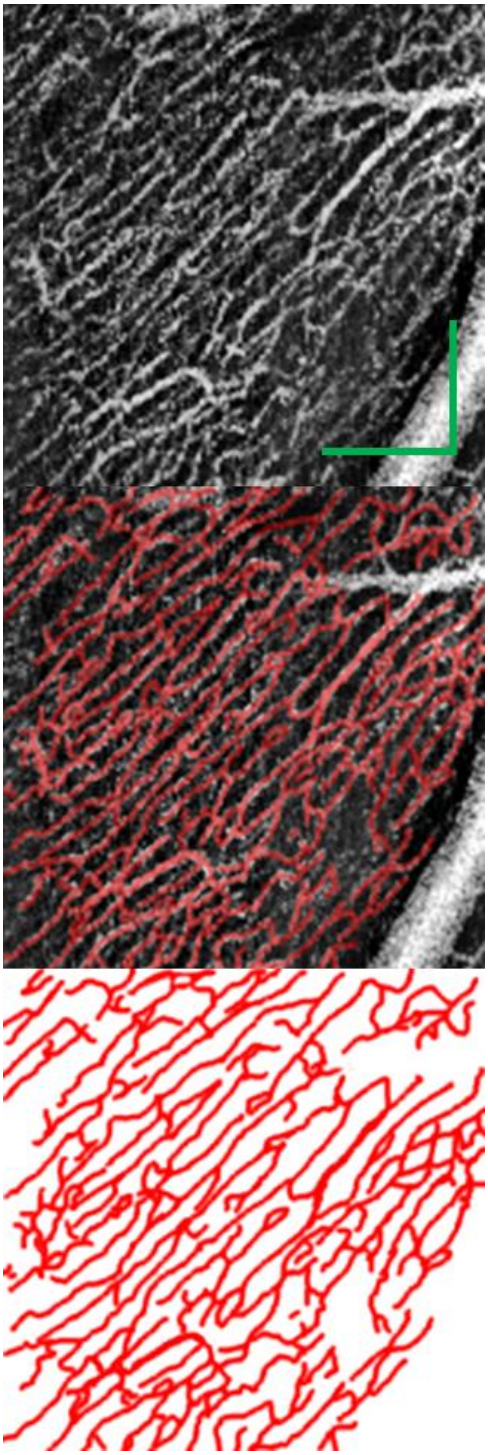

Figure 2 – **Manual tracing techniques for quantifying radial peripapillary capillary (RPC) density**. Radial peripapillary capillaries are seen in the speckle variance OCT-A image of a normal eye (Top). Manual tracing of RPCs (Center; red) were performed, the results of which were used to express the density of RPCs as a percentage of the total tissue area (Bottom). Note that large vessels were excluded from the tracing. Scale bar = 300 μm.

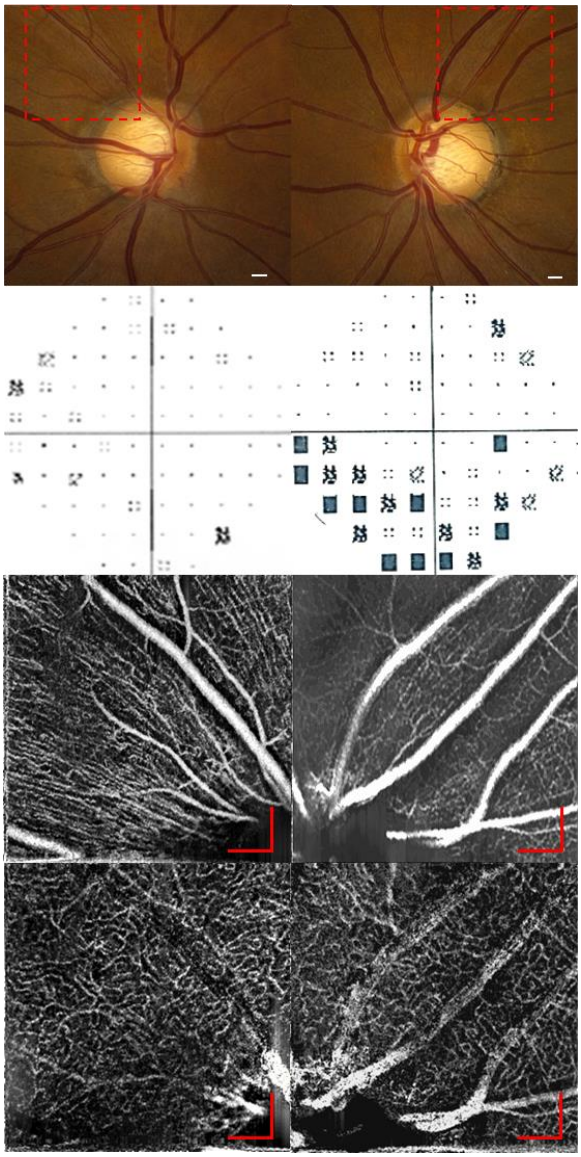

Figure 3 – **Structural changes to radial peripapillary capillaries (RPCs) in unilateral glaucoma**. The right optic disc (Top row, first image) demonstrates a myopic tilt however the automated Humphrey visual field test (Second row, first image) appears normal. Speckle variance OCT-A images of RPCs (Third row, first image) and the deep capillary plexus (Fourth row, first image) in the superotemporal peripapillary region are within the normal range. The left glaucomatous eye also demonstrates tilting (Top row, second image) but an inferior field defect is seen on visual field examination (Second row, second image). There is loss of RPCs in the superotemporal peripapillary region (Third row, second image) as seen on the speckle variance OCT-A image. The deeper capillary plexus at sites of RPC loss however appears normal and comparable in morphology to the fellow eye (Fourth row, second image). Projection artifacts from the large retinal vessels within the inner retina appear in the deeper capillary plexus images in both eyes (Fourth row, first and second image). Scale bar = 300μm.

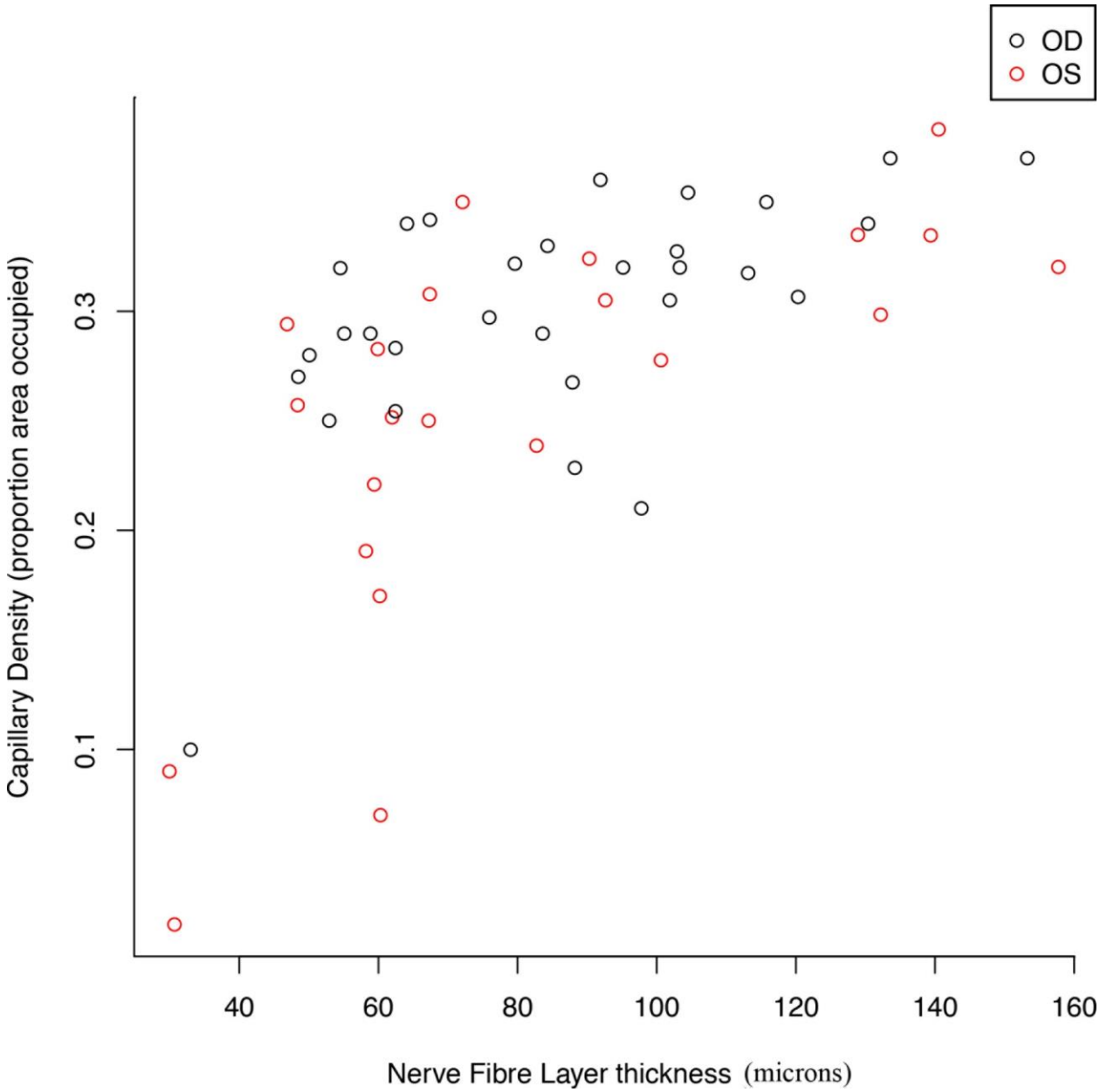

Figure 4 – Relationship between nerve fibre layer thickness and radial peripapillary capillary density using pooled data from all groups. Each data point represents a single measurement from one of the 8 peripapillary regions.

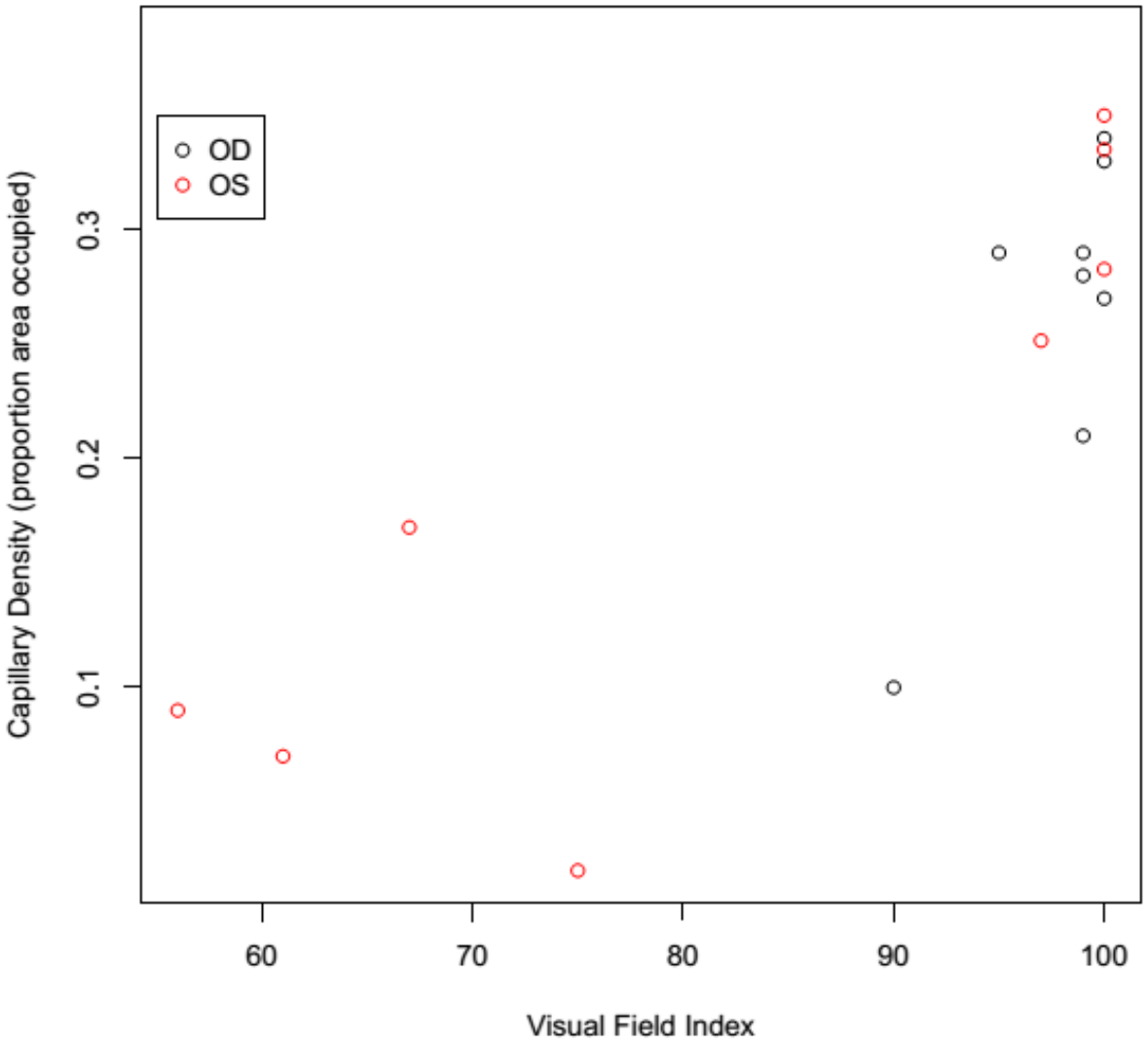

Figure 5 – **Relationship between visual field index and radial peripapillary capillary density using only subjects in groups A and B**. Each data point represents a single measurement from one of the 8 peripapillary regions.